



Published in final edited form as:

Nat Cardiovasc Res. 2022 March ; 1: 246–252. doi:10.1038/s44161-022-00035-7.

Developmental venous anomalies are a genetic primer for cerebral cavernous malformations

Daniel A. Snellings¹, Romuald Girard², Rhonda Lightle², Abhinav Srinath², Sharbel Romanos², Ying Li², Chang Chen², Aileen A. Ren³, Mark L. Kahn³, Issam A. Awad^{2,*;‡}, Douglas A. Marchuk^{1,*;‡}

¹Department of Molecular Genetics and Microbiology, Duke University School of Medicine, Durham, North Carolina 27710, USA

²Neurovascular Surgery Program, Department of Neurological Surgery, The University of Chicago Medicine and Biological Sciences, Chicago, Illinois, USA

³Department of Medicine and Cardiovascular Institute, University of Pennsylvania, 3400 Civic Center Blvd, Philadelphia PA 19104

Introductory Paragraph

Cerebral cavernous malformations (CCM) are a neurovascular anomaly that may occur sporadically, or be inherited due to autosomal dominant mutations in *KRIT1*, *CCM2*, or *PDCD10*. Individual lesions are caused by somatic mutations which have been identified in *KRIT1*, *CCM2*, *PDCD10*, *MAP3K3*, and *PIK3CA*. However, the interactions between mutations, and their relative contributions to sporadic versus familial cases remain unclear. We show that mutations in *KRIT1*, *CCM2*, *PDCD10*, and *MAP3K3* are mutually exclusive, but may co-occur with mutations in *PIK3CA*. We also find that *MAP3K3* mutations may cause sporadic, but not familial CCM. Furthermore, we find identical *PIK3CA* mutations in CCMs and adjacent developmental venous anomalies (DVA), a common vascular malformation frequently found in the vicinity of sporadic CCMs. However, somatic mutations in *MAP3K3* are found only in the CCM. This suggests that sporadic CCMs are derived from cells of the DVA which have acquired an additional mutation in *MAP3K3*.

Main Text

CCMs are prone to hemorrhage often leading to stroke, seizures and disability. The inherited form of CCM disease is characterized by numerous lesions throughout the brain and spinal

Users may view, print, copy, and download text and data-mine the content in such documents, for the purposes of academic research, subject always to the full Conditions of use: <https://www.springernature.com/gp/open-research/policies/accepted-manuscript-terms>

*Corresponding Authors: Douglas A. Marchuk (douglas.marchuk@duke.edu), Issam A. Awad (iawad@uchicago.edu).

‡Authors contributed equally

Author Contributions: DAS designed and performed the genetic studies of human CCM lesions and wrote the manuscript. IAA performed surgical resection of CCM and DVA samples used in this study. RG, RL, AS, SR, YL, CC and IAA performed plasma miRNA sequencing and analysis. AAR and MLK assisted with experimental design. RG, IAA, and DAM designed experiments and wrote the manuscript.

Competing interests: The authors declare no competing financial interests. IAA is Chairman of the Scientific Advisory Board for Angioma Alliance and provides expert opinions related to clinical care of cerebral cavernous malformations.

cord and is caused by an autosomal dominant loss of function (LOF) mutation in the genes encoding components of the CCM signaling complex: *KRIT1*^{1,2}, *CCM2*³, or *PDCD10*⁴. In contrast, sporadic CCMs typically occur as solitary lesions and form in the absence of an inherited germline mutation. Previous studies have established that somatic mutations in genes of the CCM complex cause biallelic LOF^{5–8}; however, it is unclear how the recently identified mutations in *MAP3K3* and *PIK3CA* fit into this existing model of pathogenesis.

The presence of multiple somatic mutations in CCMs also raises the question of how these mutations arise, especially in sporadic cases where none of the mutations are inherited. It has long been appreciated that sporadic CCMs often form in the vicinity of DVA, but the underlying cause has remained a long-standing mystery. DVA are the most common vascular malformation present in 6–14% of the adult population^{15–17} with the majority developing prior to the age of 20¹⁵. When assessed by magnetic resonance imaging, an adjacent DVA is identified in 24–32% of sporadic CCM cases^{12–14}, and an even greater fraction of sporadic CCMs are found to be associated with a DVA at surgery^{12,14}. One study focused on DVA reported an adjacent sporadic CCM in 6.9% of all DVAs in a general population (116 of 1689)¹⁵. These studies highlight the association between DVA and sporadic CCM. By contrast, familial CCM lesions have not been associated with DVA¹⁸. These combined data suggest that a DVA is not required for CCM formation but may be a predisposing factor in sporadic cases.

Results

To evaluate whether sporadic and familial CCMs have distinct somatic mutation spectra we identified somatic mutations present in 71 CCMs (20 familial CCMs and 51 sporadic/presumed sporadic CCMs). Familial and Sporadic CCM were identified by clinical and genetic characteristics (see Methods), whereas cases lacking information concerning family history (e.g., deidentified biobank samples) were classified as unknown. Mutations in *KRIT1*, *CCM2*, *PDCD10*, and *PIK3CA* were detected by targeted sequencing and/or droplet digital PCR (ddPCR) as previously described⁹. The common gain of function mutation in *MAP3K3* (hg38 chr17:63691212, NM_002401.3, c.1323C>G; NP_002392, p.I441M) was detected by ddPCR (Supplemental Table 1).

The p.I441M mutation in *MAP3K3* was identified in 15/51 sporadic CCMs and 0/20 familial CCMs (Figure 1A). We also screened for *MAP3K3* p.I441M in 8 blood samples for which we were previously unable to identify a germline mutation in *KRIT1*, *CCM2*, *PDCD10*. None of the 8 blood samples harbored *MAP3K3* p.I441M. Notably 11/51 sporadic CCMs harbored at least 1 somatic mutation in *KRIT1*, *CCM2*, or *PDCD10*, however none of these CCMs also had a mutation in *MAP3K3* indicating that a mutual loss of the CCM complex and gain of function in MEKK3 (the protein product of *MAP3K3*) are not both required for CCM formation. As the CCM complex is known to be a direct inhibitor of MEKK3 activity¹⁹, these data strongly suggest identical functional consequences of these mutations.

The majority of CCM and verrucous venous malformations with a mutation in *MAP3K3* harbor the p.I441M variant^{10,11,20}, however an alternative variant p.Y544H has also been

identified in a venous malformation²¹. While ddPCR provides superior sensitivity and specificity compared to targeted sequencing, it is restricted to detecting a single mutation per assay. To determine whether other mutations that contribute to CCM pathogenesis—either *MAP3K3* mutations besides p.I441M, or mutations in yet undiscovered genes—we performed whole-exome sequencing (mean depth 133×) on 8 sporadic CCMs for which no somatic mutations in *KRIT1*, *CCM2*, *PDCD10*, or *MAP3K3* were found. No additional mutations in *MAP3K3* were identified and no candidate variants in other genes passed QC filters (see Methods).

While somatic mutations in *KRIT1*, *CCM2*, *PDCD10*, and *MAP3K3* are mutually exclusive, somatic gain of function mutations in *PIK3CA* may co-occur with any other mutation (Figure 1A). We have previously shown that co-occurring mutations in *KRIT1/CCM2* and *PIK3CA* occur in the same clonal population of cells⁹. To determine whether *MAP3K3* and *PIK3CA* mutations co-exist in the same cells we performed single-nucleus DNA-sequencing (snDNA-seq) on frozen tissue from three surgically resected CCMs determined to harbor both mutations (Figure 1B–D).

In CCMs 5002 and 5030, the vast majority of mutant nuclei harbor both mutations in *MAP3K3* and in *PIK3CA* indicating that these mutations co-exist in the same cells. In CCM 5032, 37% (19/51) of mutant nuclei harbor both mutations. While this is a far lower fraction compared to other samples, it is significantly higher than may be expected by chance when sampling from 1405 total nuclei ($P = 1.3E-05$, Figure 1E). In bulk genetic analysis, the allele frequencies of *PIK3CA* and *MAP3K3* mutations detected in CCM 5002 were 19% and 13% respectively. In snDNA-seq the allele frequencies of these mutations increased to 28.7% and 30.9% respectively. This difference likely reflects the mosaic nature of CCMs. As snDNA-seq requires nuclei harvested from frozen tissue, we must sample a new area of the frozen lesion than was sampled for bulk sequencing. Sampling from different sites of the same lesion often results in minor changes in allele frequency, however the drastic change in allele frequency we find in CCM 5002 suggests either that our initial sample of the lesion for bulk sequencing contained largely non-lesion tissue, or an uneven distribution of mutant cells in the lesion.

All three samples support the coexistence of *MAP3K3* and *PIK3CA* somatic mutations in single cells, however it is worth noting that in each sample we also observe singly-mutated nuclei representing *each possible* genotype. This arrangement of mutations is biologically unlikely as it would require a somatic mutation in one gene, followed reversion of the mutation in the other gene. Instead, the observed singly-mutated genotypes are likely the result of “allelic dropout”, a common technical artifact in single-cell DNA sequencing methods²². As each allele is present in a single copy per cell, the inability to consistently amplify both alleles (e.g., due to incomplete nuclear lysis) leads to occasional, random dropout of an allele and misrepresentation of genotypes. Allelic dropout prevents us from accurately identifying the small populations of cells that acquired the first mutation prior to acquisition of the second mutation.

To determine whether DVA and CCMs originate from a shared mutation, we collected three sporadic CCMs and sampled a portion of the associated DVA obtained during surgery

(Figure 2A–C). Assays for mutations via ddPCR revealed that all three CCMs have a somatic activating mutation in *PIK3CA* and that the same mutation is present within the paired DVA samples at lower frequency (Figure 2D). Furthermore, ddPCR revealed that two of the CCMs harbored a mutation in *MAP3K3* in addition to the previously noted mutation in *PIK3CA*. However, unlike the *PIK3CA* mutation, the *MAP3K3* mutation was entirely absent from both DVA samples (Figure 2E). The presence of the *PIK3CA*, but not the *MAP3K3*, mutation in the DVA confirms that the *PIK3CA* mutation in the DVA did not arise via cross-sample contamination. The presence of multiple somatic mutations in these CCMs allows us to infer the developmental history of the lesion. The cancer field commonly uses the presence or absence of somatic mutations in clonal populations to track the evolutionary history of a tumor. Recent studies have expanded on this approach to use somatic mutations as endogenous barcodes to track embryonic development²³. Using this same approach, we infer that the DVA was the first lesion to develop and that the associated CCM is derived from cells of the DVA following a somatic mutation in *MAP3K3*. The one CCM sample in which we found a mutation in *PIK3CA* but not *MAP3K3* or CCM complex genes supports the role of *PIK3CA* in DVA development, but cannot be used to infer the temporal sequence of mutations. Notably, the lack of a *MAP3K3*/CCM complex mutation in 1 of 3 samples (33.3%) is consistent with our observations from bulk sequencing data where we did not identify *MAP3K3*/CCM complex mutations in 25 of 71 samples (35.2%).

In addition to assaying the presence of *PIK3CA* mutations in DVA associated with CCM, we would ideally also assay DVA that are not associated with CCM. Unfortunately, DVA are benign malformations and are not resected unless associated with an additional pathology. This has precluded the direct assessment of *PIK3CA* mutations in DVA without a CCM. To address this limitation, we sought another source of tissue that could be non-invasively assayed for indirect evidence of *PIK3CA* activation. Thus, we collected plasma from individuals with DVA without a CCM and measured circulating miRNAs that might serve as biomarkers reflecting *PIK3CA* activity²⁴.

We sequenced the plasma miRNomes of 12 individuals with a sporadic CCM associated with a DVA (CCM + DVA), 6 individuals with DVA only, and 7 healthy controls. Three plasma miRNAs were DE in the DVA only group when compared to healthy controls ($P < 0.05$; false discovery rate [FDR] corrected). One of the DE miRNAs, *miR-134-5p* ($\log_2(\text{FC}) = -3.30$), was downregulated and has been shown to inhibit PI3K/AKT signaling²⁵ (Supplemental Table 2).

In addition, 18 plasma miRNAs were DE in patients with DVA only when compared to CCM + DVA ($P < 0.05$; FDR corrected). One of these 18 DE miRNAs, *let-7c-5p* ($\log_2(\text{FC}) = -3.66$) was downregulated and is known to target *PIK3CA*^{26,27} (Supplemental Table 2). Of interest, *let-7c-5p* also targets *COL1A1*²⁸, a DEG within the transcriptome of human sporadic CCM lesions (see Supplemental Information).

Additionally, 28 DE plasma miRNAs were identified between CCM + DVA and healthy controls ($P < 0.05$; FDR corrected). Four of these miRNAs putatively target *PIK3CA*: *miR-148a-3p* ($\log_2(\text{FC}) = 1.71$), *miR-148b-3p* ($\log_2(\text{FC}) = 1.4$), *miR-128-3p* ($\log_2(\text{FC}) = 1.35$) and *let-7c-5p* ($\log_2(\text{FC}) = 2.07$) (Supplemental Table 2)^{26,27,29–31}.

Downregulation of a miRNA may lead to an upregulation of the targeted gene³². Even though these associations cannot be validated by somatic mutation analysis due to the lack of surgical tissue for these patients, the results of the circulating miRNome may reflect biomarkers of *PIK3CA* activation in patients harboring a DVA.

Discussion

In this study we have further interrogated the relationship between somatic mutations in *KRIT1*, *CCM2*, *PDCD10*, *MAP3K3*, and *PIK3CA* which contribute to the pathogenesis of CCM. We find that somatic mutations in *MAP3K3* are not present in CCMs from individuals with familial CCM, consistent with a recent study¹⁰. We find that sporadic CCMs may harbor mutations in *MAP3K3*, *KRIT1*, *CCM2*, or *PDCD10*, but that the lesion will only have mutations in one of these genes. This implies that mutations in any of *MAP3K3*, *KRIT1*, *CCM2*, or *PDCD10* are sufficient for CCM formation, without the need for mutations in a second gene. As the CCM complex is a direct inhibitor of *MAP3K3* activity¹⁹, this pathway may be activated by either CCM complex LOF or by *MAP3K3* GOF, but the mutual exclusivity of mutations in these genes suggests that only one of these events is necessary for lesion formation.

CCMs often develop as the result of multiple somatic mutations that co-exist within the same cells as we show with snDNA-seq. Although several somatic mutations occur in every cell division, the specificity of the mutations in CCM translates to a very low chance of acquiring these mutations within a single cell. This is especially true of somatic mutations in *MAP3K3* and *PIK3CA*, both of which have very narrow spectra of activating mutations. Despite this improbability, the accumulation of these mutations in CCM seems to occur frequently. We propose that after an initial somatic mutation, the singly-mutated cell undergoes clonal expansion to form an intermediate lesion. In this study we identify 7 CCMs with either biallelic LOF in a CCM complex gene or *MAP3K3* GOF in the absence a *PIK3CA* mutation, suggesting that *PIK3CA* activation is not required for CCM formation. Furthermore, previous work in mouse models has shown that loss of a CCM complex gene (with WT *Pik3ca*) leads to clonal expansion of the mutant cells^{33,34}. As a result of this clonal expansion, the probability of creating a double-mutant cell increases by a factor of the clonal population size as there are more cells in which the second mutation may occur. The data presented in this study suggest that DVA function similarly; developing from a *PIK3CA* mutation that clonally expands, increasing the number of cells in which a second mutation may occur.

Plasma miRNA analysis of individuals with DVA-associated CCM and DVA without CCM revealed both groups exhibit differentially expressed miRNAs that putatively target PI3K/AKT signaling. Notably, it remains unclear if the circulating DE plasma miRNAs identified herein affect their predicted gene targets and associated biological pathways *within* the lesions³⁵. While DVA only vs healthy controls revealed one DE miRNA that putatively targets PI3K/AKT signaling, DVA + CCM vs healthy controls revealed three DE miRNA targeting PI3K/AKT. This may reflect the synergistic effects of the CCM signaling pathway with *PIK3CA* mutation to drive PI3K/AKT signaling as previously reported⁹. One significant limitation of this exploratory miRNA study is the limited sample sizes of the

cohorts. While further studies will be required to understand the effects of DVA and CCM on the circulating miRNome and identify biomarkers of *PIK3CA* activation, these data are thus far consistent with our observation of *PIK3CA* gain of function mutations in DVA associated with CCM. Furthermore, these data motivate further studies to identify circulating plasma miRNAs that may be a valuable clinical tool to non-invasively assay *PIK3CA* activation.

The presence of *PIK3CA* mutations in DVA suggests that DVA act as a genetic precursor to CCM, which would account for the strong association between sporadic CCM and DVA (Figure 3). Likewise, DVA are not associated with familial CCM because the presence of an inherited germline mutation in a CCM gene biases probability towards a CCM gene somatic mutation occurring first, as there exist many different mutations that may cause LOF, but far fewer that would cause GOF in *PIK3CA*.

Collecting tissue from CCM-associated DVA is challenging; however, collecting tissue from DVA not associated with CCM is yet more challenging as DVA are considered benign and are therefore not resected. We have attempted to address this limitation by studying biomarkers of PI3K activity which can be assayed noninvasively in blood plasma. Assaying the presence of *PIK3CA* mutations in DVA not associated with CCM will be the domain of future studies, but the data we present here demonstrate a clear link between DVA and *PIK3CA*, and suggest a model that explains the long recognized—but poorly understood—association between CCM and DVA.

While we are unable to address the presence of *PIK3CA* mutations in DVA not associated with CCM, it is worth noting that DVAs have been associated with other PI3K-related disorders^{36–39,40} including some cancers and neurological malformations, suggesting that DVA may have a role, possibly even as a genetic primer, in these other phenotypes.

Methods

Sample Collection

Surgically resected CCMs were obtained from consenting participants at the University of Chicago, the Barrow Neurological Institute, and the Angioma Alliance biobank. Additional DVA tissue was discretely dissected from the lesion during surgical resection of the associated CCM at the University of Chicago. This study was approved by each institution's respective Institutional Review Board.

Familial and Sporadic Diagnosis

Familial-CCM patients harbor multiple lesions throughout the brain on MR susceptibility weighted imaging (SWI), a documented CCM1, CCM2, or CCM3 germline mutation, and/or first-degree relative with a history of CCM. Sporadic/solitary patients typically harbor a single lesion on SWI, or a cluster of CAs associated with a developmental venous anomaly⁴¹. Cases without clear information about family history—e.g., deidentified samples acquired from tissue biobanks—were classified as unknown.

DNA Extraction

DNA from CCM and DVA samples was extracted using the DNeasy blood and tissue kit (QIAGEN, catalog number 69504) per the manufacturers protocol. DNA purity was determined by Nanodrop and concentration was determined using the Qubit dsDNA BR assay kit (Invitrogen, catalog number Q32850) per the manufacturers protocol.

Droplet Digital PCR

Detection of *MAP3K3* p.I441M was performed via ddPCR using a previously published probe set²⁰ detailed and synthesized by Integrated DNA Technologies.

Forward Primer: 5'-TGCAGTACTATGGCTGTCTG-3'

Reverse Primer: 5'-GTCTCACATGCATTCAAGG-3'

Reference Allele Probe: 5'-HEX-CCTGACCATcTTCATGGAGTACA-IBlk-3'

Alternate Allele Probe: 5'-FAM-CCTGACCATgTTCATGGAGTACA-IBlk-3'

Assays were performed using 30–100ng of DNA with the QX200 AutoDG system (BioRad) and quantified with the QX200 droplet reader (BioRad). Analysis was performed with the QuantaSoft software (BioRad).

Sequencing

A total of 8 sporadic CCMs with no identified mutation in *KRIT1*, *CCM2*, *PDCD10*, or *MAP3K3* (5001, 5005, 5006, 5022, 5024, 5036, 5078, and 5081) were used for whole-exome sequencing prepared using the SureSelect Human All Exon V7 probe set (Agilent, Design ID S31285117) per the manufacturers protocol. Prepared libraries were sequenced on one lane of a NovaSeq 6000 S4 flow cell for a mean depth of 133×.

Sequence Analysis

Sequencing data was processed using the Gene Analysis Toolkit (GATK, Broad Institute) while following the GATK best practices for somatic short variant discovery using Mutect2. Secondary variant detection was performed using [gnomics](https://github.com/vertgenlab/gonomics) (<https://github.com/vertgenlab/gonomics>) and bcftools mpileup to manually examine *KRIT1*, *CCM2*, *PDCD10*, and *MAP3K3* for somatic variants. Putative variants were annotated using Funcotator (GATK), the catalog of somatic mutation in cancer (COSMIC), and the genome aggregation database (gnomAD). Putative variants were filtered according to the following criteria: greater than 50× total coverage, less than 90% strand specificity, greater than 5 reads supporting the alternate allele, greater than 1% alternate allele frequency, less than 1% population allele frequency, and predicted protein/splicing change.

Single-Nucleus DNA Sequencing

Nuclei isolates were prepared via Dounce homogenization of frozen tissue in Nuclei EZ Lysis Buffer (Sigma-Aldrich) and sorted to a single-nucleus suspension with a FACSAriaII (BD) (70um nozzle, 70psi, 4-Way Purity, chiller). Sequencing libraries from individual nuclei were prepared using the Tapestry platform (MissionBio) using a custom panel

targeting *KRIT1*, *CCM2*, *PDCD10*, *MAP3K3*, and *PIK3CA*. Libraries were pooled and sequenced with a NextSeq Mid-Output 2×150bp kit (Illumina). Data processing and QC was performed with the MissionBio cloud analysis pipeline (v1.10.0). P values for mutation co-occurrence was determined by χ^2 test of observed and expected genotype counts as determined by a Poisson distribution⁹.

miRNA Extraction and Sequencing

Total plasma RNA was extracted from the plasma of 12 individuals with a sporadic CCM and an associated DVA (CCM + DVA), 6 individuals with DVA and without a CCM (DVA only), and 7 healthy controls using the miRNeasy Serum/Plasma Kit (Qiagen, Hilden, Germany) following the manufacturer isolation protocol. Diagnosis of CCM with an associated DVA, as well as DVA without a CCM lesion was confirmed on susceptibility weighted MR imaging. Illumina small RNA-Seq kits (Clontech, Mountain View, CA, USA) were then used to generate cDNA libraries, and sequencing was completed with the Illumina HiSeq 4000 platform (Illumina, San Diego, CA, USA), with single-end 50bp reads, at the University of Chicago Genomics Core. Differential miRNA analyses were completed between (1) CCM + DVA to DVA only and then (2) DVA only to healthy controls. The differentially expressed miRNAs were identified having $P < 0.05$, FDR-corrected. All analyses were completed using the sRNAToobox and DESeq2 R packages^{42,43}.

Identification of Putative Targets

miRWalk 3.0 was queried to identify the putative gene targets of each of the DE miRNAs, using a random forest tree algorithm with a bonding prediction probability higher than 95% on the 3 different gene locations (3' UTR, 5' UTR, and CDS)⁴⁴. Putative gene targets of the DE miRNAs were identified in at least 2 of the 3 databases. DE miRNAs between (1) CCM + DVA and DVA only as well as (2) DVA only and healthy controls were then analyzed for potential targeting of the PI3K signalling pathway.

Data Availability:

Data not included in this paper can be accessed through NCBI (DNA sequencing, BioProject Accession: PRJNA802805) or GEO (RNA sequencing, Accession: GSE195732). Public datasets used here are available at COSMIC (cancer.sanger.ac.uk/cosmic), dbSNP (ncbi.nlm.nih.gov/snp), 1000 Genomes Project (internationalgenome.org), ExAC (gnomad.broadinstitute.org), miRWalk3.0 (mirwalk.umm.uni-heidelberg.de) and the DAVID database (david.ncifcrf.gov).

Code availability:

Variant calling software was implemented as part of Gonomics, an ongoing effort to develop an open-source genomics platform in the Go programming language. Gonomics can be accessed at github.com/vertgenlab/gonomics.

Supplementary Material

Refer to Web version on PubMed Central for supplementary material.

Acknowledgements:

We thank the patients who donated tissue for this study. We thank Angioma Alliance, the Barrow Neurological Institute, and the University of Chicago for patient enrollment and sample collection. Nucleus sorting was performed in the Duke Human Vaccine Institute Research Flow Cytometry Shared Resource Facility. We thank Duke University School of Medicine for use of the Sequencing and Genomic Technologies Shared Resource for library preparation and sequencing. These studies were supported by National Institute of Health grants, P01NS092521 (DM, IA, MK), F31HL152738 (DS).

References

1. Laberge-le Couteulx S et al. Truncating mutations in CCM1, encoding KRIT1, cause hereditary cavernous angiomas. *Nat Genet* 23, 189–193, doi:10.1038/13815 (1999). [PubMed: 10508515]
2. Sahoo T et al. Mutations in the gene encoding KRIT1, a Krev-1/rap1a binding protein, cause cerebral cavernous malformations (CCM1). *Hum Mol Genet* 8, 2325–2333, doi:10.1093/hmg/8.12.2325 (1999). [PubMed: 10545614]
3. Liquori CL et al. Mutations in a gene encoding a novel protein containing a phosphotyrosine-binding domain cause type 2 cerebral cavernous malformations. *Am J Hum Genet* 73, 1459–1464, doi:10.1086/380314 (2003). [PubMed: 14624391]
4. Bergametti F et al. Mutations within the programmed cell death 10 gene cause cerebral cavernous malformations. *Am J Hum Genet* 76, 42–51, doi:10.1086/426952 (2005). [PubMed: 15543491]
5. Gault J, Shenkar R, Recksiek P & Awad IA Biallelic somatic and germ line CCM1 truncating mutations in a cerebral cavernous malformation lesion. *Stroke* 36, 872–874, doi:10.1161/01.STR.0000157586.20479.fd (2005). [PubMed: 15718512]
6. Gault J et al. Cerebral cavernous malformations: somatic mutations in vascular endothelial cells. *Neurosurgery* 65, 138–144; discussion 144–135, doi:10.1227/01.NEU.0000348049.81121.C1 (2009). [PubMed: 19574835]
7. Akers AL, Johnson E, Steinberg GK, Zabramski JM & Marchuk DA Biallelic somatic and germline mutations in cerebral cavernous malformations (CCMs): evidence for a two-hit mechanism of CCM pathogenesis. *Hum Mol Genet* 18, 919–930, doi:10.1093/hmg/ddn430 (2009). [PubMed: 19088123]
8. McDonald DA et al. Lesions from patients with sporadic cerebral cavernous malformations harbor somatic mutations in the CCM genes: evidence for a common biochemical pathway for CCM pathogenesis. *Hum Mol Genet* 23, 4357–4370, doi:10.1093/hmg/ddu153 (2014). [PubMed: 24698976]
9. Ren AA et al. PIK3CA and CCM mutations fuel cavernomas through a cancer-like mechanism. *Nature* 594, 271–276, doi:10.1038/s41586-021-03562-8 (2021). [PubMed: 33910229]
10. Weng J et al. Somatic MAP3K3 mutation defines a subclass of cerebral cavernous malformation. *Am J Hum Genet* 108, 942–950, doi:10.1016/j.ajhg.2021.04.005 (2021). [PubMed: 33891857]
11. Hong T et al. Somatic MAP3K3 and PIK3CA mutations in sporadic cerebral and spinal cord cavernous malformations. *Brain*, doi:10.1093/brain/awab117 (2021).
12. Abdulrauf SI, Kaynar MY & Awad IA A comparison of the clinical profile of cavernous malformations with and without associated venous malformations. *Neurosurgery* 44, 41–46; discussion 46–47, doi:10.1097/00006123-199901000-00020 (1999). [PubMed: 9894962]
13. Wurm G, Schnizer M & Fellner FA Cerebral cavernous malformations associated with venous anomalies: surgical considerations. *Neurosurgery* 57, 42–58; discussion 42–58, doi:10.1227/01.neu.0000163482.15158.5a (2005).
14. Porter PJ, Willinsky RA, Harper W & Wallace MC Cerebral cavernous malformations: natural history and prognosis after clinical deterioration with or without hemorrhage. *J Neurosurg* 87, 190–197, doi:10.3171/jns.1997.87.2.0190 (1997). [PubMed: 9254081]
15. Brinjikji W, El-Rida El-Masri A, Wald JT & Lanzino G Prevalence of Developmental Venous Anomalies Increases With Age. *Stroke* 48, 1997–1999, doi:10.1161/STROKEAHA.116.016145 (2017). [PubMed: 28536179]
16. Linscott LL, Leach JL, Jones BV & Abruzzo TA Developmental venous anomalies of the brain in children -- imaging spectrum and update. *Pediatr Radiol* 46, 394–406; quiz 391–393, doi:10.1007/s00247-015-3525-3 (2016). [PubMed: 26795616]

17. Gokce E, Acu B, Beyhan M, Celikyay F & Celikyay R Magnetic resonance imaging findings of developmental venous anomalies. *Clin Neuroradiol* 24, 135–143, doi:10.1007/s00062-013-0235-9 (2014). [PubMed: 24240482]
18. Dammann P et al. Correlation of the venous angioarchitecture of multiple cerebral cavernous malformations with familial or sporadic disease: a susceptibility-weighted imaging study with 7-Tesla MRI. *J Neurosurg* 126, 570–577, doi:10.3171/2016.2.JNS152322 (2017). [PubMed: 27153162]
19. Zhou Z et al. The cerebral cavernous malformation pathway controls cardiac development via regulation of endocardial MEKK3 signaling and KLF expression. *Dev Cell* 32, 168–180, doi:10.1016/j.devcel.2014.12.009 (2015). [PubMed: 25625206]
20. Couto JA et al. A somatic MAP3K3 mutation is associated with verrucous venous malformation. *Am J Hum Genet* 96, 480–486, doi:10.1016/j.ajhg.2015.01.007 (2015). [PubMed: 25728774]
21. Al-Qattan MM et al. Late-onset multiple venous malformations confined to the upper limb: link to somatic MAP3K3 mutations. *J Hand Surg Eur Vol* 45, 1023–1027, doi:10.1177/1753193420922459 (2020).
22. Xu L et al. Clonal Evolution and Changes in Two AML Patients Detected with A Novel Single-Cell DNA Sequencing Platform. *Sci Rep* 9, 11119, doi:10.1038/s41598-019-47297-z (2019). [PubMed: 31366893]
23. Bizzotto S et al. Landmarks of human embryonic development inscribed in somatic mutations. *Science* 371, 1249–1253, doi:10.1126/science.abe1544 (2021). [PubMed: 33737485]
24. Mori MA, Ludwig RG, Garcia-Martin R, Brandao BB & Kahn CR Extracellular miRNAs: From Biomarkers to Mediators of Physiology and Disease. *Cell Metab* 30, 656–673, doi:10.1016/j.cmet.2019.07.011 (2019). [PubMed: 31447320]
25. Yang C et al. Exosome miR-134–5p restrains breast cancer progression via regulating PI3K/AKT pathway by targeting ARHGAP1. *J Obstet Gynaecol Res* 47, 4037–4048, doi:10.1111/jog.14983 (2021). [PubMed: 34378285]
26. Yuan H et al. MicroRNA let-7c-5p promotes osteogenic differentiation of dental pulp stem cells by inhibiting lipopolysaccharide-induced inflammation via HMGA2/PI3K/Akt signal blockade. *Clin Exp Pharmacol Physiol* 46, 389–397, doi:10.1111/1440-1681.13059 (2019). [PubMed: 30575977]
27. Li Y, Li P & Wang N Effect of let-7c on the PI3K/Akt/FoxO signaling pathway in hepatocellular carcinoma. *Oncol Lett* 21, 96, doi:10.3892/ol.2020.12357 (2021). [PubMed: 33376529]
28. Srivastava SP, Hedayat AF, Kanasaki K & Goodwin JE microRNA Crosstalk Influences Epithelial-to-Mesenchymal, Endothelial-to-Mesenchymal, and Macrophage-to-Mesenchymal Transitions in the Kidney. *Front Pharmacol* 10, 904, doi:10.3389/fphar.2019.00904 (2019). [PubMed: 31474862]
29. Yin H et al. MiR-148a-3p Regulates Skeletal Muscle Satellite Cell Differentiation and Apoptosis via the PI3K/AKT Signaling Pathway by Targeting Meox2. *Front Genet* 11, 512, doi:10.3389/fgene.2020.00512 (2020). [PubMed: 32582277]
30. Cimino D et al. miR148b is a major coordinator of breast cancer progression in a relapse-associated microRNA signature by targeting ITGA5, ROCK1, PIK3CA, NRAS, and CSF1. *FASEB J* 27, 1223–1235, doi:10.1096/fj.12-214692 (2013). [PubMed: 23233531]
31. Huo L et al. miR-128–3p inhibits glioma cell proliferation and differentiation by targeting NPTX1 through IRS-1/PI3K/AKT signaling pathway. *Exp Ther Med* 17, 2921–2930, doi:10.3892/etm.2019.7284 (2019). [PubMed: 30906475]
32. Correia de Sousa M, Gjorgjieva M, Dolicka D, Sobolewski C & Foti M Deciphering miRNAs' Action through miRNA Editing. *Int J Mol Sci* 20, doi:10.3390/ijms20246249 (2019).
33. Detter MR, Snellings DA & Marchuk DA Cerebral Cavernous Malformations Develop Through Clonal Expansion of Mutant Endothelial Cells. *Circ Res* 123, 1143–1151, doi:10.1161/CIRCRESAHA.118.313970 (2018). [PubMed: 30359189]
34. Malinverno M et al. Endothelial cell clonal expansion in the development of cerebral cavernous malformations. *Nat Commun* 10, 2761, doi:10.1038/s41467-019-10707-x (2019). [PubMed: 31235698]
35. Turchinovich A, Samatov TR, Tonevitsky AG & Burwinkel B Circulating miRNAs: cell-cell communication function? *Front Genet* 4, 119, doi:10.3389/fgene.2013.00119 (2013). [PubMed: 23825476]

36. Roux A et al. High Prevalence of Developmental Venous Anomaly in Diffuse Intrinsic Pontine Gliomas: A Pediatric Control Study. *Neurosurgery* 86, 517–523, doi:10.1093/neuros/nyz298 (2020). [PubMed: 31342064]
37. Brinjikji W et al. Facial Venous Malformations Are Associated with Cerebral Developmental Venous Anomalies. *AJNR Am J Neuroradiol* 39, 2103–2107, doi:10.3174/ajnr.A5811 (2018). [PubMed: 30237297]
38. Tan WH et al. The spectrum of vascular anomalies in patients with PTEN mutations: implications for diagnosis and management. *J Med Genet* 44, 594–602, doi:10.1136/jmg.2007.048934 (2007). [PubMed: 17526801]
39. Dhamija R et al. Neuroimaging abnormalities in patients with Cowden syndrome: Retrospective single-center study. *Neurol Clin Pract* 8, 207–213, doi:10.1212/CPJ.0000000000000463 (2018). [PubMed: 30105160]
40. Rasalkar DD & Paunipagar BK Developmental venous anomaly associated with cortical dysplasia. *Pediatr Radiol* 40 Suppl 1, S165, doi:10.1007/s00247-010-1654-2 (2010). [PubMed: 20429001]
41. Akers A et al. Synopsis of Guidelines for the Clinical Management of Cerebral Cavernous Malformations: Consensus Recommendations Based on Systematic Literature Review by the Angioma Alliance Scientific Advisory Board Clinical Experts Panel. *Neurosurgery* 80, 665–680, doi:10.1093/neuros/nyx091 (2017).
42. Rueda A et al. sRNAtoolbox: an integrated collection of small RNA research tools. *Nucleic Acids Res* 43, W467–473, doi:10.1093/nar/gkv555 (2015). [PubMed: 26019179]
43. Love MI, Huber W & Anders S Moderated estimation of fold change and dispersion for RNA-seq data with DESeq2. *Genome Biol* 15, 550, doi:10.1186/s13059-014-0550-8 (2014). [PubMed: 25516281]
44. Sticht C, De La Torre C, Parveen A & Gretz N miRWalk: An online resource for prediction of microRNA binding sites. *PLoS One* 13, e0206239, doi:10.1371/journal.pone.0206239 (2018).

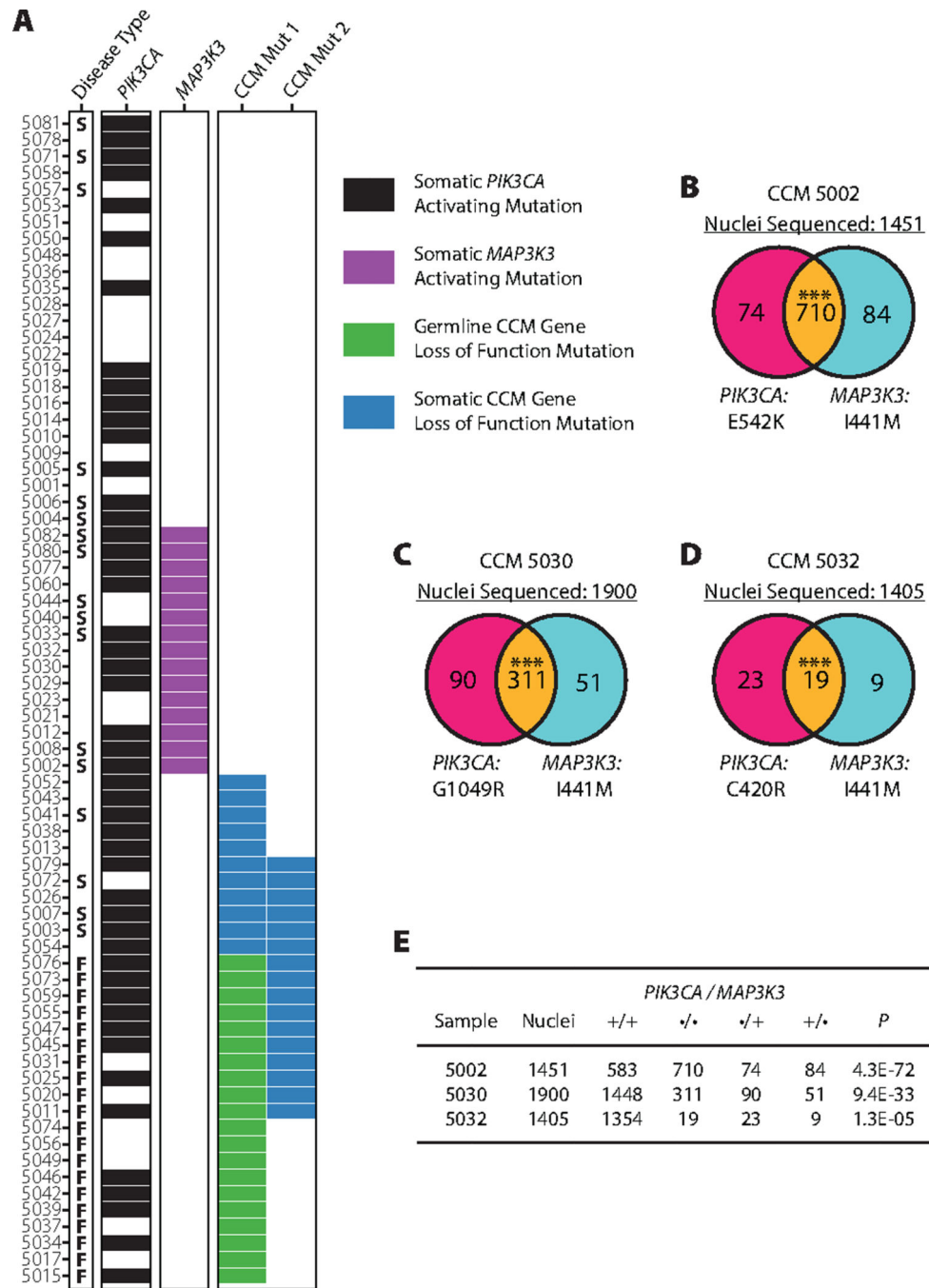


Figure 1. Mutations in *MAP3K3* are mutually exclusive with CCM gene mutations and occur in the same cells as *PIK3CA* mutations.

A. Mutations present in 71 cerebral cavernous malformations (CCMs). Disease type denotes whether the sample was familial (F), sporadic (S), or unknown (blank). The presence of somatic mutations in *PIK3CA* and *MAP3K3* are denoted by black and purple bars respectively. Germline and somatic mutations (green and blue respectively) in *KRIT1*, *CCM2*, or *PDCD10*, are shown in CCM Mut 1 with the second-hit mutation shown in CCM Mut 2 if present. **B-D.** Nuclei genotypes determined by snDNA-seq. The left and right

circles in each Venn diagram shows the number of nuclei with the *PIK3CA* or *MAP3K3* mutations where the overlap shows nuclei harboring both mutations. *** $P < 0.0001$, $P = 4.3E-27$ (B), $9.4E-33$ (C), $1.3E-05$ (D). **E.** Summary of data presented in B-D including P values determined by χ^2 of the observed number of double mutant nuclei to the expected value derived from a Poisson distribution as done previously⁹.

Author Manuscript

Author Manuscript

Author Manuscript

Author Manuscript

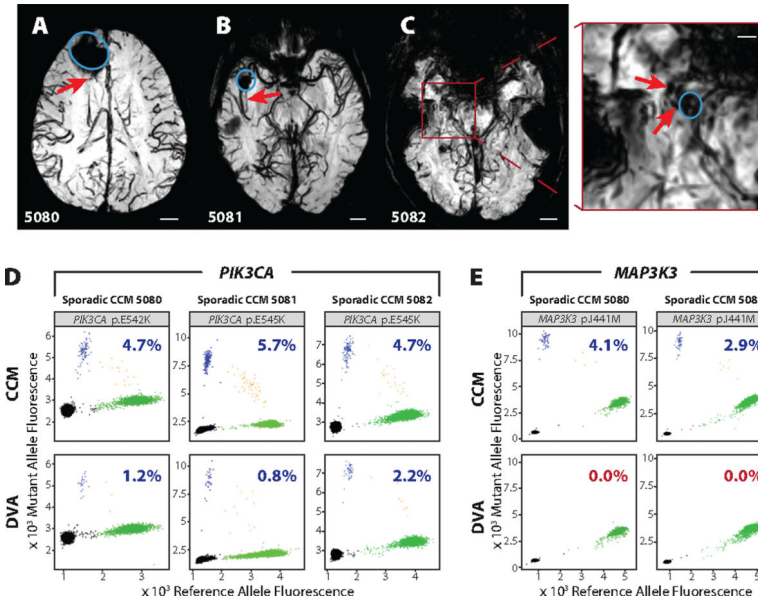


Figure 2. Associated CCM and DVA harbor identical somatic mutations in *PIK3CA*.
A, B, C. Axial magnetic resonance (MR) susceptibility weighted images acquired at 3 Tesla showing CCM (blue circle) and associated DVA branches sampled during surgery (red arrow) in individuals with cerebral cavernous malformation (CCM) 5080 (A) or 5081 (B) or 5082(C) (scale bars 15mm). The inset red box in C shows the region expanded to the right with the CCM and developmental venous anomaly (DVA) marked (scale bar 5mm). **D, E.** Somatic mutations in *PIK3CA* (D) and *MAP3K3* (E) in CCM (top panels) and the associated DVA (bottom panels) from samples 5081, 5082, and 5083. Mutations were detected by droplet digital PCR and shown as the fluorescence of the reference probe on the x-axis, and the mutant probe on the y-axis. Droplets containing the reference allele, mutant allele, both, or neither, are colored in green, blue, orange, and black respectively. Percentage inset into each graph shows the variant allele frequency for the displayed mutation. If the mutation was determined to be present, the percentage is blue, else the percentage is red.

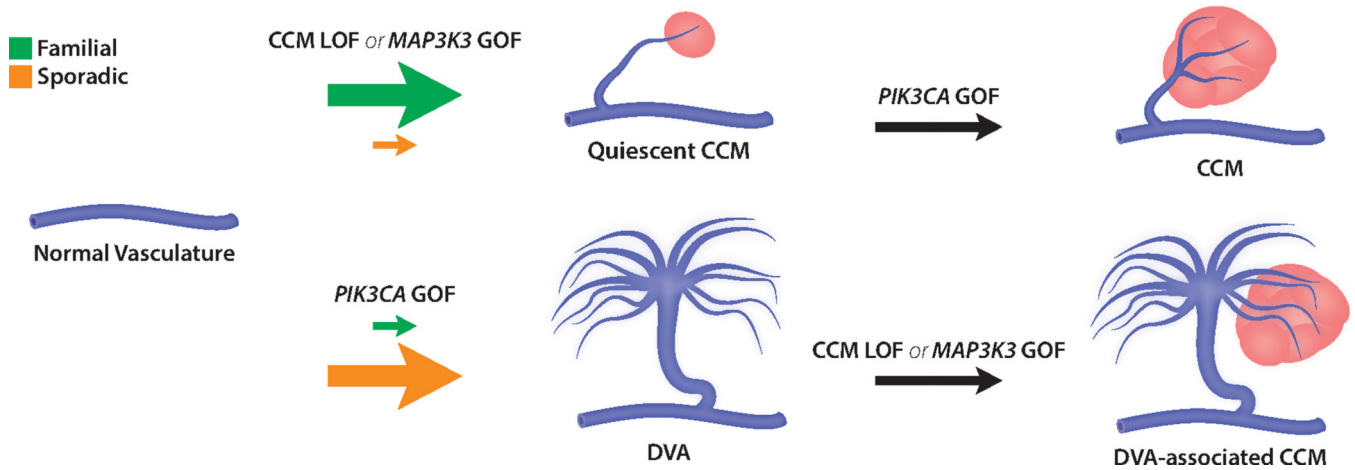


Figure 3. Genetic model of CCM pathogenesis.

The genetic trajectories that underly familial and sporadic cerebral cavernous malformation (CCM) pathogenesis. Familial CCMs already harbor a predisposing germline mutation in the CCM complex (*KRIT1*, *CCM2*, *PDCD10*) and are therefore most likely to develop without requiring association with a developmental venous anomaly (DVA) (top). In contrast, individuals without familial CCM—but who have a *PIK3CA*-mutant DVA—are predisposed to sporadic CCM formation adjacent to the DVA as one genetic ‘hit’ is already present (bottom). However, sporadic CCMs could also develop in the absence of the DVA (top), depending on the temporal sequence of acquisition of somatic mutations. GOF, gain of function; LOF, loss of function.